Characterizing crystalline polymorph transitions in HfO_2 by extended x-ray absorption fine-structure spectroscopy

Patrick S. Lysaght[a)]
SEMATECH, 2706 Montopolis Drive, Austin, Texas 78741-6499, USA

Joseph C. Woicik
National Institute of Standards and Technology, Gaithersburg, Maryland 20899, USA

M. Alper Sahiner
Physics Department, Seton Hall University, 400 S. Orange Avenue, South Orange, New Jersey 07079, USA

Byoung-Hun Lee
SEMATECH, 2706 Montopolis Drive, Austin, Texas 78741-6499, USA

Raj Jammy
IBM Assignee, SEMATECH, 2706 Montopolis Drive, Austin, Texas 78741-6499, USA

(Received 31 July 2007; accepted 31 August 2007; published online 19 September 2007)

Atomic layer deposited HfO_2 films on Si(100) substrates have been measured by extended x-ray absorption fine-structure (EXAFS), pre- and postanneal processing. Analysis of the second coordination shell indicates an increase in atomic order with increasing film thickness for each anneal temperature and with increasing anneal temperature for each film thickness. Fourier transformed EXAFS spectra fit with HfO_2 reference phases have identified orthorhombic to tetragonal to monoclinic transformations. Evidence for greater retention of the higher permittivity metastable tetragonal phase corresponding to thinner HfO_2 films is consistent with a surface energy effect giving rise to the critical grain size phenomenon. © *2007 American Institute of Physics*.
[DOI: 10.1063/1.2789180]

An industry wide effort to incorporate a thin Hf-based high-k ($k \approx 12-25$) gate dielectric film to replace SiO_2 ($k=3.9$) and maintain the prescribed rate of device scaling[1] has given rise to electrical performance enhancements due to improved chemical engineering of thin dielectric films.[2] High resolution spectroscopic techniques capable of characterizing subtle film and interface stoichiometric variations as a function of gate stack layer deposition and subsequent anneal processing have emerged as critical requirements for the identification of microstructure driven mechanisms that limit or enhance the electrical performance of Hf-based complementary metal oxide semiconductor devices.[3]

HfO_2 blanket thin films were produced by atomic layer deposition (ALD) via precursor material tetrakis(ethylmethylamino)hafnium with ozone oxidation, TEMAHf+O_3, on Si(100) substrates at 330 °C, while the target HfO_2 thickness was achieved, based on a growth rate of ~0.08 nm/cycle. Kirsch *et al.*[4] determined the scaling limit of HfO_2 to be 15 ALD cycles ($T_{phys}=1.2\pm0.2$ nm), where electrical results concur with physical evidences (x-ray reflectivity density, low energy ion scattering continuity, and x-ray photoelectron spectroscopy chemical states), indicating that 1.2 nm films begin to deviate from bulk HfO_2 properties. Transistors exhibit an improvement in both peak and high field mobility as HfO_2 thickness scales from 3.3 to 1.2 nm, which is likely due to reduced charge trapping and reduced Coulomb scattering. These results underscore the need for high resolution physical characterization to elucidate microstructure variations corresponding to performance advantages of aggressively scaled HfO_2 films. To that end, extended x-ray absorption fine-structure (EXAFS) spectroscopy measurements have been performed on a series of scaled thickness, uncapped HfO_2 blanket films (T_{phys}=1.4, 1.8, and 4.0 nm), following each of the three standard device thermal processing cycles: (i) as deposited at 330 °C, (ii) postdeposition anneal (PDA) of 700 °C for 60 s in NH_3 ambient at 30 Torr, and (iii) PDA plus rapid thermal anneal (RTA) at 1000 °C for 5 s in N_2 ambient at atmospheric pressure. EXAFS is well suited for probing local structural distortions in thin HfO_2 films as a function of anneal processing since the technique is sensitive to correlations on a length scale of a few angstroms.[5]

The experiment was performed at the National Synchrotron Light Source at Brookhaven National Laboratory on beamline X23A2, operated by the National Institute of Standards and Technology. The Hf L_3 absorption edge (9561 eV) was used in the EXAFS data acquisition in the fluorescence detection mode with a 5° angle of x-ray incidence. The $\chi(k)$ functions were obtained by subtracting the atomic absorption background using the AUTOBK code.[6] The resultant functions were Fourier transformed (FT) using a Gaussian window set for 2.0–12.5 $Å^{-1}$ k range. Analysis of the FT data provides information on the near-neighbor coordination, distance, and the local disorder around the absorbing Hf atom obtained using the University of Washington developed multiple scattering EXAFS calculation code FEFF8.4.[7]

The cubic (c) HfO_2 phase has a fluorite-type structure (space group F_{3m3}), in which each Hf^{4+} ion is coordinated by eight equidistant O^{2-} ions and each O^{2-} ion is tetrahedrally coordinated by four Hf^{4+} ions.[8,9] The reference c-HfO_2 phase[10,11] did not produce a good fit with any of the FT spectra of this sample set. Figure 1(a) illustrates a set of FEFF8.4 calculated FT scattering path functions corresponding

[a)]Author to whom correspondence should be addressed. Electronic mail: pat.lysaght@sematech.org

 © 2007 American Institute of Physics
Downloaded 22 May 2008 to 10.1.150.90. Redistribution subject to AIP license or copyright; see http://apl.aip.org/apl/copyright.jsp

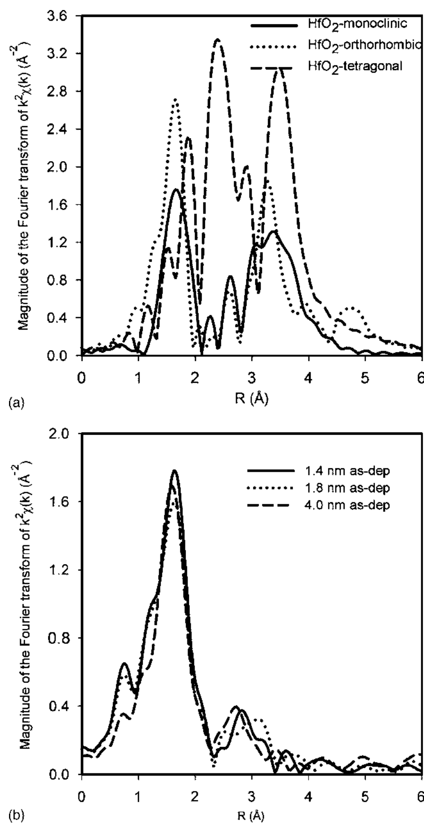

FIG. 1. (a) The reference FEFF8.4 calculated monoclinic, orthorhombic, and tetragonal phases of HfO_2 and (b) the Fourier transformed EXAFS data for 1.4, 1.8, and 4.0 nm thick HfO_2 prior to anneal processing (330 °C deposition temperature).

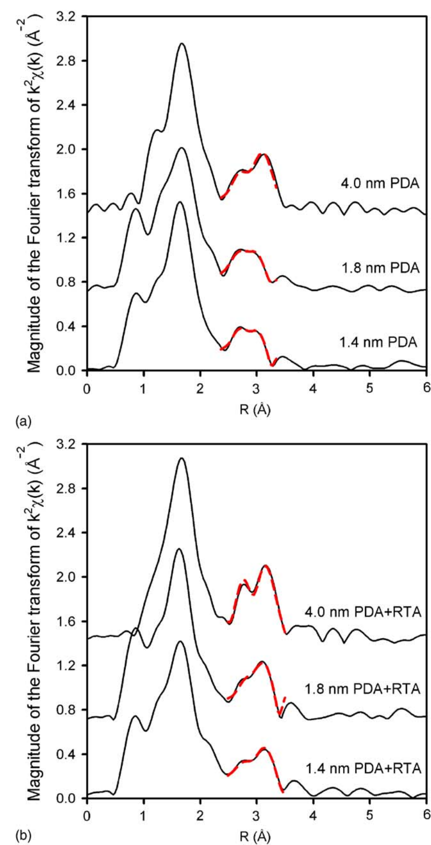

FIG. 2. (Color online) The Fourier transformed EXAFS data for 1.4, 1.8, and 4.0 nm thick HfO_2 (a) following the PDA process of 700 °C for 60 s in NH_3 ambient and (b) following the PDA (700 °C for 60 s in NH_3) + RTA (1000 °C for 10 s in N_2 ambient) process.

to monoclinic (m),[12,13] tetragonal (t),[13,14] and orthorhombic (o)[15,16] phases of HfO_2 which were used to identify the polymorphs contributing to the FT data. These references have been rendered for pure phases with theoretical coordination numbers, without Debye-Waller factors. Although the peak intensities differ from experimental data, the location and shape offer valid phase identification comparisons. Figure 1(b) illustrates the FT EXAFS data for 1.4, 1.8, and 4.0 nm thick HfO_2 prior to anneal processing ($T_{\text{deposition}}=330$ °C). It is difficult to interpret the second order peaks conclusively since they all appear amorphous, and definitive order in these thin as-deposited films is not expected.

The temperature, pressure, and anneal ambient definitely affect the polymorphism of HfO_2. The sevenfold coordination structure of m-HfO_2 (space group $P2_1/c$) consists of triangularly coordinated O_I–Hf^{3+} and tertahedrally coordinated O_{II}–Hf^{4+}, while t-HfO_2 (space group $P4_2/nmc$) resembles a distorted fluorite-type cubic structure with Hf^{4+} surrounded by eight O^{2-} ions.[14] For the first coordination shell peak of the 4.0 nm HfO_2 PDA film at ~1.8 Å radial distance in Fig. 2(a), Hf–O scattering amplitude and phase were used to model the spectra which correspond to seven nearest neighbor O atoms in m-HfO_2. The double-peak feature at ~3 Å radial distance in the calculated m-HfO_2 structure in Fig. 1(a) is clearly evident in the 4.0 nm HfO_2 PDA film. Fitting this sample yields a bimodal microstructure fractions of 0.67 monoclinic and 0.33 tetragonal which are consistent with previously reported x-ray diffraction (XRD) plots of 3 nm HfO_2 exposed to the N incorporating NH_3 PDA process.[17] The second shell fitting data in Table I illustrate the influence of HfO_2 thickness on the resultant polymorph, and no match with m-HfO_2 was detected for the 1.4 and 1.8 nm HfO_2 PDA films which fit t-HfO_2 with only a slight fraction of orthorhombic. It has been reported that the high pressure (~2–15 GPa) o-HfO_2 polymorph (cotunnite-type) could be preserved,[14,18] however, it does not exist in equilibrium and is rarely encountered within the process parameters associated with transistor thin film fabrication. The second shell peak at ~3.0 Å is sensitive to crystal symmetry variations and is dominated by Hf–Hf backscattering.[19] Multiple scattering from Hf–O–O paths was found to be negligible.

The results of the second shell fitting of FT EXAFS spectra correlated with monoclinic, tetragonal, and orthorhombic polymorphs as a function of thickness and anneal processing are indicated in Table I and overlaid on the second shell of the FT spectra shown in Figs. 2(a) and 2(b). Figure 2(a) illustrates a tetragonal to monoclinic transformation (for films annealed at the same temperature and pressure) corresponding to film thickness (grain size dependence). This transformation is martensitic in nature, whereby the change in crystal structure is diffusionless, achieved by a homogeneous deformation of the parent phase into the product phase.[20,21] It has been shown that HfO_2 is strongly anisotropic in thermal expansion, with the b axis exhibiting negligible expansion, while the expansion is substantial for the a and c axes and the phase transition is athermal, occurring over a temperature range, i.e., the amount of the transformed phase varies with change in temperature but not as a function of time at a particular temperature.[14] Figure 2(b) illustrates the FT EXAFS spectra of HfO_2 PDA+RTA (1000 °C for 10 s in N_2 ambient) films. The 4.0 nm HfO_2 PDA+RTA

Downloaded 22 May 2008 to 10.1.150.90. Redistribution subject to AIP license or copyright; see http://apl.aip.org/apl/copyright.jsp

TABLE I. Second shell fittings of Fourier transformed EXAFS spectra of HfO_2 indicates correlation with monoclinic, tetragonal, and orthorhombic phases as a function of thickness and anneal processing. The uncertainties in the near-neighbor distances and the coordination numbers are ±0.01 and ±0.1 Å, respectively.

Sample ID	Second shell fits: Monoclinic ($P2_1/c$) R_{Hf-Hf} (Å)	Monoclinic N_{Hf-Hf}	Tetragonal ($P4_2/nmc$) R_{Hf-Hf} (Å)	Tetragonal N_{Hf-Hf}	Orthorhombic ($Pbca$) R_{Hf-Hf} (Å)	Orthorhombic N_{Hf-Hf}
1.4 nm PDA			3.38	10.3	3.44	5.4
1.8 nm PDA			3.57	10.9	3.44	5.7
4.0 nm PDA	3.51	6.5	3.7	9.8		
1.4 nm PDA+RTA	3.49	6.5	3.68	10.2		
1.8 nm PDA+RTA	3.47	6.2	3.65	9.9		
4.0 nm PDA+RTA	3.37	6.7	3.64	9.6		

sample was nearly identical to a measured m-HfO_2 reference powder sample (that was fitted as m-HfO_2 with a volume fraction of 1.0). The Hf–Hf coordination increases (greater degree of crystallization) and the monoclinic fraction increases with HfO_2 thickness. There is a critical grain size (~4–10 nm) for the tetragonal to monoclinic transformation, below which the tetragonal phase may be retained at temperatures sufficient to produce m-HfO_2 in slightly thicker films with slightly larger grains.[22]

Although XRD (short-range order limit of ~4–5 nm) and high resolution transmission electron microscopy images in plan view and cross section suggest that the 1.4 nm HfO_2 samples of Figs. 2(a) and 2(b) remain amorphous following RTA, EXAFS data in Table II clearly identify evidence of t-HfO_2 for the PDA sample and coexistence of m-HfO_2 (57%) and t-HfO_2 (43%) for the PDA+RTA sample. A plausible explanation is that the short-range order identified in the EXAFS spectra corresponds to a HfO_2 grain size that is below the detection sensitivity of XRD. This indicates that the volume fraction of order and the grain size decrease with decreasing film thickness due to surface energy effects which are consistent with the retention of t-HfO_2 following PDA. Although the monoclinic phase is suppressed for the 1.4 and 1.8 nm HfO_2 PDA samples, each thickness exhibits evidence of m-HfO_2 following PDA+RTA annealing, such that the fraction of monoclinic phase increases with film thickness. The fraction of each polymorph corresponding to annealed HfO_2 films was accurately determined from the second shell fitting and is listed in Table II.

Consider the electrical performance of aggressively scaled nanocrystalline HfO_2 gate dielectric films. There is an appreciable advantage in retaining the higher permittivity tetragonal phase in terms of further equivalent oxide thickness (EOT) scaling, given the current minimum thickness limit of ~1.2 nm for deposition of a continuous layer. Furthermore, since the ratio of t-HfO_2 (k=28–29) to m-HfO_2 (k=16–18) is shown to increase as the film is scaled thinner, more accurate assessment of the contribution from the interfacial SiO_x layer to the composite EOT is achievable. Now that characterization of capacitor and transistor devices comprised of sub-2-nm high-k dielectric films has become commonplace, it is critical to assume the appropriate fraction of t-HfO_2 that will directly lead to a more precise estimate of the permittivity contribution and corresponding quality of the SiO_x interface between the HfO_2 and the Si substrate (k=3.9 for stoichiometric SiO_2 and k=11.9 for α-Si) and avoid possible exaggeration of oxygen deficiency due to an overestimate of the SiO_x k value.

TABLE II. Volume fractions of monoclinic, tetragonal, and orthorhombic HfO_2 as a function of thickness and anneal processing.

	Fraction: Monoclinic	Tetragonal	Orthorhombic
1.4 nm PDA	0	0.96	0.04
1.8 nm PDA	0	0.99	0.01
4.0 nm PDA	0.67	0.33	0
1.4 nm PDA+RTA	0.57	0.43	0
1.8 nm PDA+RTA	0.6	0.4	0
4.0 nm PDA+RTA	0.96	0.04	0

This work has been supported by Research Corporation Award No. CC6405 and NSF Award No. DMI-0420952.

[1] International Technology Roadmap for Semiconductors, 2005.
[2] M. A. Quevedo-Lopez, S. A. Krishnan, P. D. Kirsch, G. Pant, B. E. Gnade, and R. M. Wallace, Appl. Phys. Lett. **87**, 262902 (2005).
[3] P. S. Lysaght, J. Barnett, J. C. Woicik, B. Foran, G. Bersuker, and B.-H. Lee, ECS Trans. **1**, 313 (2006).
[4] P. D. Kirsch, M. A. Quevedo-Lopez, H.-J. Li, Y. Senzaki, J. J. Peterson, S. C. Song, S. A. Krishnan, N. Moumen, J. Barnett, G. Bersuker, P. Y. Hung, B. H. Lee, T. Lafford, Q. Wang, D. Gay, and J. G. Ekerdt, J. Appl. Phys. **99**, 023508 (2006).
[5] B. Ravel, Y.-I. Kim, P. M. Woodward, and C. M. Fang, Phys. Rev. B **73**, 184121 (2006).
[6] M. Newville, P. Livins, Y. Yacoby, J. J. Rehr, and E. A. Stern, Phys. Rev. B **47**, 14126 (1993).
[7] A. L. Ankudinov, B. Ravel, J. J. Rehr, and S. D. Conradson, Phys. Rev. B **58**, 7565 (1998).
[8] D. K. Smithand and C. F. Cline, J. Am. Ceram. Soc. **45**, 249 (1962).
[9] A. A. Demkov and X. Zhang, Proceedings of the IEEE International Symposium on Compound Semiconductors 2000 (unpublished), p. 155.
[10] R. Ramprasad and N. Shi, Phys. Rev. B **72**, 052107 (2005).
[11] A. A. Demkov, Phys. Status Solidi B **226**, 57 (2001).
[12] R. E. Hahn, P. R. Suitch, and J. L. Pentecost, J. Am. Ceram. Soc. **68**, C–285 (1985).
[13] X. Zhao and D. Vanderbilt, Phys. Rev. B **65**, 233106 (2002).
[14] J. Wang, H. P. Li, and R. Stevens, J. Mater. Sci. **27**, 5397 (1992).
[15] J. E. Jaffe, R. A. Bachorz, and M. Gutowski, Phys. Rev. B **72**, 144107 (2005).
[16] S. Desgreniers and K. Lagarec, Phys. Rev. B **59**, 8467 (1999).
[17] P. S. Lysaght, J. Woicik, D. Fischer, G. I. Bersuker, J. Barnett, B. Foran, H.-H. Tseng, and R. Jammy, J. Appl. Phys. **101**, 024105 (2007).
[18] L. Liu, J. Phys. Chem. Solids **41**, 331 (1980).
[19] M. A. Sahiner, J. C. Woicik, P. Gao, P. McKeown, M. C. Croft, M. Gartman, and B. Benapfl, Thin Solid Films **515**, 6548 (2007).
[20] G. M. Wolten, J. Am. Ceram. Soc. **46**, 418 (1963).
[21] A. H. Heuer and M. Ruhle, Acta Metall. **33**, 2101 (1985).
[22] R. C. Garvie, J. Phys. Chem. **69**, 1238 (1965).

Downloaded 22 May 2008 to 10.1.150.90. Redistribution subject to AIP license or copyright; see http://apl.aip.org/apl/copyright.jsp